Bauschinger effect in unpassivated freestanding nanoscale metal films

Jagannathan Rajagopalan, Jong H. Han and M. Taher A. Saif*

Department of Mechanical Science and Engineering, University of Illinois at Urbana-Champaign, Urbana, IL 61801, USA

We show experimentally that unpassivated freestanding nanoscale metal films, subjected to uniaxial tension, show substantial Bauschinger effect (BE) during unloading, even at large overall tensile stresses. Aluminum films (thickness 200–400 nm, grain size ≈200 nm) show BE at stresses as high as 150 MPa and their plastic strain after unloading is often less than 50% of the expected value. In gold, BE is relatively smaller. Possible mechanisms for BE in unpassivated thin metal films are discussed.
© 2008 Acta Materialia Inc. Published by Elsevier Ltd. All rights reserved.

Keywords: Thin films; Plastic deformation; Bauschinger effect

Thin metal films, because of their unique dimensional and microstructural constraints, exhibit a substantially different mechanical response compared to their bulk, coarse-grained counterparts [1–5]. The yield stress of these films is, for example, often an order of magnitude larger than bulk metals, but their ductility is much lower [6,7]. Various theoretical models, including strain-gradient plasticity [8–10] and crystal plasticity theories [11], have been proposed and discrete dislocation simulations [12–14] performed to describe thin film plasticity. These theories, at least qualitatively, explain the strengthening effects associated with film thickness and grain size. Some of the theoretical models [15] and simulations [11] also predict a distinct Bauschinger effect (BE) in passivated thin films upon unloading. BE [16,17] refers to the reduction in yield stress of a material during reverse straining after being plastically deformed in the forward direction. These models and simulations show that the stress–strain response of passivated metal films deviates from elastic behavior during unloading, even when the films are still under tension.

Predictions of BE in passivated films have found support in various experimental studies [18–21] that have revealed early yielding in thin metal films on substrates during thermomechanical cycling. Early yielding in these passivated films has normally been attributed to the presence of stored dislocation energy, which assists reverse plastic deformation during unloading. Energy gets stored during the forward deformation because the dislocations are prevented from exiting the film by the passivation layer, resulting in dislocation pile-ups [12] or misfit dislocation segments being deposited [22] at the film/passivation layer interface. In the absence of a passivation layer, dislocations are free to exit the film and hence it is accepted that unpassivated films should not show early yielding. Even recent experiments [23,24] that provided direct evidence of BE in passivated thin metal films did not reveal any BE in similar unpassivated films. We show experimentally that unpassivated free-standing metal films, but with smaller thicknesses and grain sizes compared to films examined in the above studies, exhibit a distinct BE during unloading. These films, which were deformed under pure uniaxial tension, show large deviations from linear elastic behavior during unloading even at high values of overall tensile stress.

Aluminum films of thickness 210, 360 and 400 nm and a gold film of thickness 240 nm were sputter deposited directly on bare silicon wafers. From these films several free-standing aluminum and gold tensile specimens were co-fabricated with microelectromechanical system-based tensile testing chips using the process described in Ref. [25]. The films are labeled based on their thickness (Al-210, for example, denotes the 210 nm thick Al film) and these labels are used to refer them in the manuscript. The microstructure of these films were examined using transmission electron microscopy (TEM), cross-sectional

* Corresponding author. Tel.: +1 217 333 8552; e-mail: saif@uiuc.edu

scanning electron microscopy (SEM) and X-ray diffraction (XRD). The mean grain size was measured using plan-view TEM for the aluminum films and cross-sectional SEM for the gold films. The Al-210 film typically had one grain across the thickness whereas the other films had two grains. TEM images showed a large grain size distribution in the aluminum films, with grains ranging from 60 to 400 nm. The microstructural details of the films are summarized in Table 1. The table also shows the ratio of free surface to grain boundary (GB) area for an average grain in the films.

In the experiments, both loading and unloading were done quasi-statically. The specimens were subjected to small increments/decrements in strain and the deformation was then halted for a period of one minute, after which the stress–strain data was recorded. The aluminum and gold free-standing specimens tested in this study were 10–15 μm wide and 300–800 μm long. For all the films, at least two specimens were tested to ensure repeatability of the observations. The strain and stress resolutions were better than 0.005% and 4 MPa for measurements on the aluminum specimens. The corresponding values for the gold specimens were 0.005% and 5 MPa, respectively.

A brief description of the notations used in this paper for quantifying the BE is shown in Figure 1. Here, ϵ represents the total strain during loading, ϵ_p the expected plastic strain if the specimen traced an elastic unloading path and ϵ_B the recovered strain (the difference between the expected and actual plastic strain). σ_y and σ_{yr} denote the forward and reverse yield stresses, respectively. Both σ_y and σ_{yr} are determined by the point of deviation from elastic behavior. The lower the σ_{yr}, that is, earlier the deviation from elastic behavior during unloading, the higher the ϵ_B and hence the BE.

The stress–strain response of two Al-210 specimens is shown in Figure 2. In cycle 1, the first specimen (Fig. 2a) was deformed to 0.67% strain and unloaded. During unloading, the initial slope was ≈70 GPa, the bulk elastic modulus. However, as the unloading progressed,

Table 1. Mean grain size (d) and texture ($\perp$) to film surface of the films tested in this study

Film	d (nm)	Texture	Free surface to GB area
Al-210	170	(1 0 0) and (1 1 1)	0.405
Al-360	200	(1 0 0) and (1 1 1)	0.217
Al-400	190	(1 0 0) and (1 1 1)	0.192
Au-240	80	(1 1 1)	0.143

In the aluminum films, both the textures were weak. The free surface to GB area listed is for an average grain in the films.
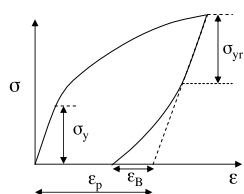
Figure 1. Description of notations used for quantifying BE. A lower σ_{yr} leads to larger ϵ_B and hence a more pronounced BE.
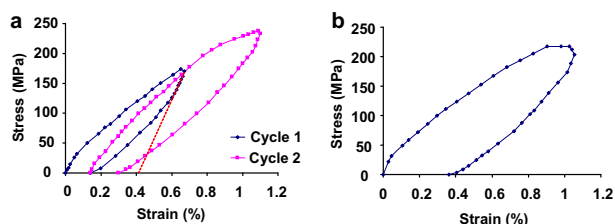
Figure 2. (a) Stress–strain curves during two deformation cycles of a 210 nm thick aluminum specimen showing a pronounced BE. (b) Loading and unloading response of another 210 nm thick aluminum specimen, which was deformed to higher strains.

there was a pronounced reduction in the stress–strain slope. The final plastic strain was just 0.14% as opposed to the expected plastic strain (ϵ_p) of 0.42%. In other words, the recovered strain (ϵ_B) was 0.28%. During the second loading ($\epsilon = 0.96\%$, $\epsilon_p = 0.62\%$), the specimen exhibited slight residual hardening and recovered an even larger fraction ($\epsilon_B/\epsilon_p = 0.74\%$) of plastic strain during unloading. After the second unloading, the specimen was annealed at 220 °C for 20 min to check for strain recovery, but none was observed.

To explore the behavior at higher strains, we deformed the second specimen up to a strain of 1.05% and unloaded (Fig. 2b). This specimen also showed a small yield stress and substantial hardening. However, at about 0.9% strain, the specimen started flowing plastically, that is, there was no stress increase with increasing strain, which was followed by a small stress drop. During unloading early yielding was again observed ($\epsilon_B = 0.38\%$), but the percentage of recovered strain was lower ($\epsilon_B/\epsilon_p = 0.52$). TEM observations of both the specimens showed no noticeable change in the grain size after deformation.

Similar experiments performed on the Al-360 specimens (grain size 200 nm) showed that their stress–strain response (Fig. 3) was broadly similar to the Al-210 specimens. These specimens also showed no grain growth during deformation and no strain recovery after unloading. However, there were some differences. The forward yield stress, for example, was higher whereas the magnitude of BE was lower. In the Al-400 specimens (data not shown), BE was larger compared to the Al-360 specimens.

To ascertain whether other face-centered cubic metals exhibited BE, we performed similar experiments on gold specimens (thickness 240 nm, grain size 80 nm) for two reasons. One, unlike aluminum, gold films do not have
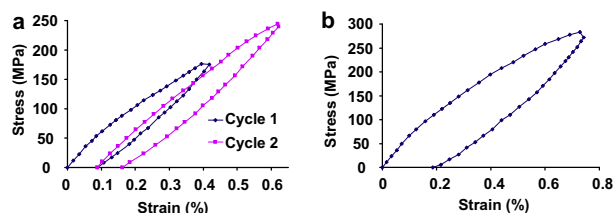
Figure 3. (a) Stress–strain response of a 360 nm thick aluminum specimen. The BE was larger during the second cycle, where the specimen was subjected to higher stresses. (b) The response of another 360 nm thick aluminum specimen, showing that the stress–strain slope reduces markedly at higher strains.

a native oxide layer on the surface, which could act as a passivation layer. Secondly, gold films typically have a strong (1 1 1) texture in the film growth direction. Experiments on two representative gold specimens (Fig. 4) confirmed the presence of BE. The magnitude of BE was quite small with reverse yielding occurring at lower stresses (Fig. 4a) compared to the aluminum films. But the specimens showed substantial strain recovery after unloading upon annealing, unlike the aluminum films (Fig. 4b).

A conceptual mechanism that could lead to BE in unpassivated thin metal films is shown in Figure 5. The figure shows the stresses in a large and two surrounding smaller grains at two points, A and B, during loading and unloading, respectively. The large grain is representative of grains that are favorably oriented for plastic deformation while the smaller grains are symbolic of grains that undergo little plastic activity. During loading, the large grain starts deforming plastically at low stresses whereas the smaller grains accommodate the strain elastically. As the external load is increased, the stress in the smaller grains keep increasing. However, the stress in the larger grain remains low (no hardening from dislocation entanglements) as the dislocations can escape to the surface. This leads to a highly inhomogeneous stress distribution in the film. Furthermore, once the larger grains start deforming plastically the stress–strain slope reduces markedly – the apparent strain hardening observed in our specimens is most likely the manifestation of such inhomogeneous (elastic and plastic) deformation. The hypothesis that many dislocations escape to the surface is supported by ex situ TEM observations of the deformed Al-210 specimens which show very few dislocations even in larger grains.

During the initial stages of unloading both the large and the smaller grains unload elastically. However, as the unloading progresses, the large grain goes into compression as it was under much smaller stress at the start of unloading. This compressive stress leads to reverse plastic deformation in the larger grain (the dislocations are of opposite sign now) and hence BE. In Figure 5, the dislocations are shown to emanate from an intragranular source merely for convenience; the dislocations could originate from the grain boundaries as well.

Based on the above mechanism, the internal stress acting on the large (plastically deforming) grains should be proportional to the difference between the maximum stress during loading (σ_{max}) and the yield stress (σ_y). As this internal stress provides the driving force for reverse
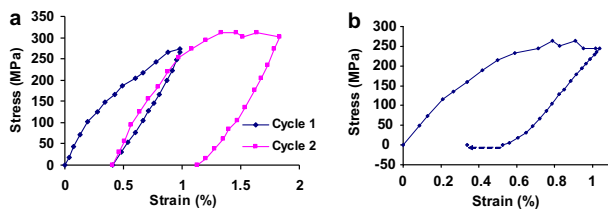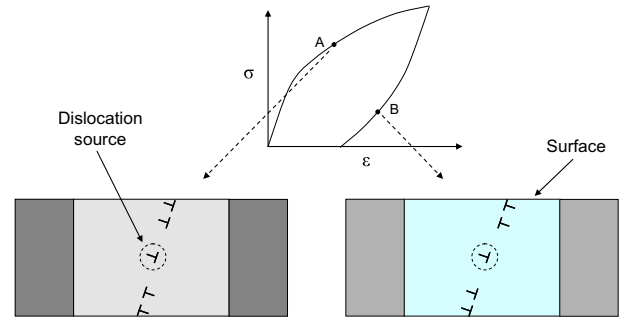
Figure 5. A conceptual mechanism for BE in metal films with columnar grains. The figure shows the stresses in a large and two surrounding smaller grains. Grey and blue colors indicate tensile and compressive stress while darker shades represent higher magnitude. During loading (A), the large grain has lower stress as it deforms plastically. During unloading (B), the large grain undergoes reverse plastic deformation even though the overall stress is still tensile. (For interpretation of the references to colour in this figure legend, the reader is referred to the web version of this article.)

plastic deformation during unloading, ϵ_B should have a direct correlation with $\sigma_{max} - \sigma_y$. A plot of ϵ_B vs $\sigma_{max} - \sigma_y$ normalized by the Young's modulus, E (Fig. 6), shows that ϵ_B monotonically increases with $(\sigma_{max} - \sigma_y)/E$ for all three films. A direct comparison across the films is not possible because of their different grain size, structure and thickness. However, note that the Al-210 film, where more dislocations can escape to the surface because of the larger free surface to GB area ratio (Table 1), shows the maximum ϵ_B.

In the discussions so far, BE has been attributed to the inhomogeneous stress distribution caused by grain size variations. However, other factors, like variations in texture, could be responsible as well. Baker et al. [26], for example, found that in unpassivated Cu films subjected to thermomechanical cycling, the average stress in (1 1 1) oriented grains was about 3.8 times the average stress in (1 0 0) oriented grains. In other words, plastic deformation in (1 1 1) grains was substantially less compared to (1 0 0) grains. If this were true for aluminum films as well, it would lead to large stress variations in the films tested here as they have both (1 0 0) and (1 1 1) oriented grains. The BE seen in the aluminum films could, at least in part, be the result of such texture induced stress variations. On the other hand, inhomogeneous stress distributions can also be caused by pile-up of dislocations at grain boundaries. If such pile-ups occur, the back stresses arising from them can lead to early yielding [27]. However, if this were the primary mechanism, the magnitude of BE would have been higher in the thicker aluminum films and the gold

Figure 4. (a) Stress–strain response of a 240 nm thick gold specimen, showing reverse yielding during unloading. (b) The response of another gold specimen, which was annealed at 160 °C for 10 min after unloading. The specimen showed noticeable strain recovery (indicated by the dashed arrow) upon annealing.
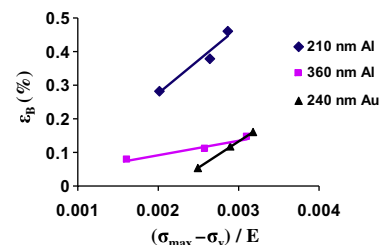
Figure 6. Plot of ϵ_B vs $(\sigma_{max} - \sigma_y)/E$ for the gold and aluminum films, indicating a direct correlation between the two quantities.

film (which have a relatively larger GB area), which is contrary to our observations.

Our results unambiguously show that unpassivated free-standing metal films exhibit BE. However, the mechanism responsible for BE in unpassivated films seems vastly different from that in passivated films. In passivated films, blockage of dislocations by the passivation layer leads to BE. In unpassivated films the selective plastic relaxation of larger/favourably oriented grains, coupled with elastic accommodation in smaller/unfavorably oriented grains, appears to be the cause. Note that the films examined in most previous studies on BE [18,20,21,23] were thicker and had substantially larger grain sizes compared to the films tested here. At larger mean grain sizes, one would expect plastic deformation and hence the stress distribution to be more homogeneous, unless dislocations are prevented from exiting the film. Therefore, one does not expect thicker unpassivated films to show BE.

Although there have been no previous reports of BE in unpassivated metal films, recent investigations [28] have revealed substantial plastic strain recovery in gold and aluminum thin films (thickness 200 nm, grain size 50–65 nm) after unloading. This time-dependent strain recovery was attributed to the combination of small grain size and inhomogeneous deformation. However, the aluminum films tested in this study, which have larger grain sizes ($d \approx 200$ nm) compared to the films studied in Ref. [28], exhibit BE but no strain recovery after unloading.

This change in behavior, we hypothesize, is due to the following reason. At smaller d (≈ 50 nm) intragranular dislocation sources are scarce and hence dislocations mostly initiate from grain boundaries. These dislocations are pinned by grain boundary structures like ledges during their propagation and require thermal activation to depin and propagate further [29]. Therefore, apart from internal stresses, thermal activation is required for reverse plastic deformation to occur, which leads to time-dependent strain recovery after unloading [???]. At larger d (like the aluminum films studied here) dislocations generated from intragranular dislocation sources are more likely to dominate plasticity. These dislocations are less likely to be pinned by grain boundary structures during their propagation and hence their propagation is largely athermal, that is, there is less time dependence. Hence, reverse plasticity occurs during unloading, leading to BE. However, if the unloading rate is very high, the internal stresses may not fully relax during unloading and some strain recovery may occur after unloading.

The results described here and in Ref. [28] together indicate that, at small mean grain sizes, microstructural variations such as differences in size and texture of individual grains could greatly influence the macroscopic behavior of metal films. Hence, in understanding the plastic behavior of ultrafine-grained and nanocrystalline thin metal films it is necessary to take into account microstructural variations and the inhomogeneous stress distributions they produce.

Supplementary data associated with this article can be found, in the online version, at doi:10.1016/j.scriptamat.2008.06.010.

[1] W.D. Nix, Metall. Trans. A 20 (A) (1989) 2217.
[2] R. Venkatraman, J.C. Bravman, J. Mater. Res. 7 (1992) 2040.
[3] E. Arzt, Acta Mater. 46 (1998) 5611.
[4] R.-M. Keller, S.P. Baker, E. Arzt, Acta Mater. 47 (1999) 415.
[5] H. Huang, F. Spaepen, Acta Mater. 48 (2000) 3261.
[6] M.A. Haque, M.T.A. Saif, Sens. Actuators A 97–98 (2002) 239.
[7] Y.M. Wang, K. Wang, D. Pan, K. Lu, K.J. Hemker, E. Ma, Scr. Mater. 48 (2003) 1581.
[8] E.C. Aifantis, Int. J. Engng. Sci. 30 (10) (1992) 1279.
[9] H. Gao, Y. Huang, W.D. Nix, J.W. Hutchinson, J. Mech. Phys. Solids 47 (6) (1999) 1239.
[10] N.A. Fleck, J.W. Hutchinson, J. Mech. Phys. Solids 49 (2001) 2245.
[11] E. Bittencourt, A. Needleman, M. Gurtin, E. Van der Giessen, J. Mech. Phys. Solids 51 (2003) 281.
[12] L. Nicola, E. Van der Giessen, A. Needleman, J. Appl. Phys. 93 (2003) 5920.
[13] H.D. Espinosa, S. Berbenni, M. Panico, K.W. Schwarz, Proc. Natl. Acad. Sci. USA 102 (2005) 1693316938.
[14] L. Nicola, Y. Xiang, J. Vlassak, E. Van der Giessen, A. Needleman, J. Mech. Phys. Solids 54 (2006) 20892110.
[15] S. Yefimov, I. Groma, E. Van der Giessen, J. Mech. Phys. Solids 52 (2004) 279.
[16] R. Sowerby, D.K. Uko, Y. Tomita, Mater. Sci. Eng. 41 (1979) 43.
[17] T. Hasegawa, T. Yakou, U.F. Kocks, Mater. Sci. Eng. 81 (1986) 189.
[18] C. Volkert, C.F. Alofs, J.R. Liefting, J. Mater. Res. 9 (1994) 1147.
[19] R. Keller, S.P. Baker, E. Arzt, J. Mater. Res. 13 (1998) 1307.
[20] R.P. Vinci, S.A. Forrest, J.C. Bravman, J. Mater. Res. 17 (2002) 1863.
[21] S.P. Baker, R.-M. Keller-Flaig, J.B. Shu, Acta Mater. 51 (2003) 3019.
[22] S.P. Baker, R.-M. Keller, E. Arzt, Mater. Res. Soc. Symp. Proc. 505 (1998) 605.
[23] Y. Xiang, J.J. Vlassak, Scr. Mater. 53 (2005) 177.
[24] Y. Xiang, J.J. Vlassak, Acta Mater. 54 (2006) 5449.
[25] J.H. Han, M.T.A. Saif, Rev. Sci. Instrum. 77 (2006) 045102.
[26] S.P. Baker, A. Kretschmann, E. Arzt, Acta Mater. 49 (2001) 2145.
[27] H.D. Espinosa, M. Panico, S. Berbenni, K.W. Schwarz, Inter. J. Plas. 22 (2006) 2091.
[28] J. Rajagopalan, J.H. Han, M.T.A. Saif, Science 315 (2007) 1831.
[29] H. Van Swygenhoven, P.M. Derlet, A.G. Froseth, Acta Mater. 54 (2006) 1975.
[30] J. Rajagopalan, J.H. Han, M.T.A. Saif, Scripta Mater. (2008), doi:10.1016/j.scriptamat.2008.02.060.